Major Depressive Disorder Is Associated with Abnormal Interoceptive Activity and Functional Connectivity in the Insula

Supplemental Information

Table of Contents

Supplemental Methods

Additional Imaging Task Details

After the resting scan, but prior to the start of the Focused Awareness scans, we presented to each subject a three-minute practice version of the task while they lay in the scanner. This shortened practice version of the task included all interoceptive and exteroceptive conditions present within the full task, as well as rating periods for all task conditions. We observed participants throughout these practice sessions and ensured both that they were able to use the scroll-wheel to make responses and that they fully understood the requirements of the task itself.

In each of the three functional magnetic resonance imaging (fMRI) task scanning runs, we presented the task conditions in a pseudo-random order optimized for fMRI analysis by Optseq2 (http://surfer.nmr.mgh.harvard.edu/optseq/). Each condition trial was separated by a variable-duration interstimulus interval lasting between 2.5 and 22.5-seconds (mean interval = 6.7 seconds), during which time subjects saw only a black fixation mark against a white background. Stimuli were projected onto a screen located inside the scanner bore and viewed through a mirror system mounted on the head-coil. We controlled stimulus presentation and response collection using Eprime2 software (www.pstnet.com). Upon entering the scanner, subjects first underwent a 7 minute 30 second resting-state fMRI scan, during which they viewed a black fixation-cross presented against a white background. We instructed subjects to focus on the fixation-cross, and that for the duration of the resting scan they were simply to clear their mind and not think of anything in particular.

Heart Rate Analysis

We analyzed the pulse oximetry recordings for the resting and Focused Awareness task scans using the suite of 1D analysis tools available within the AFNI software package as follows. For each 10-second period during the scans (45 during the resting scan, and 55 during each Focused Awareness task scan), we normalized the pulse oximetry recording to a maximum intensity of 1 within the 10-second window and raised the intensity values to the 4th power, in order to account for low-level noise

within the recorded signal. We then calculated the derivative of the signal to isolate local signal peaks and multiplied the output by a step function to isolate time points with a positive slope. The result was a binary output with a '1' representing each individual heartbeat within the 10-second window. We subsequently calculated the average R-R distance (the time between individual heart beats) within each 10-second period and averaged the resulting values to obtain the mean R-R distance for each scan. We then divided the number corresponding to the pulse oximeter sampling frequency (50 hz x 60 seconds = 3000) by the average R-R distance to obtain the average heart rate throughout the scan. The output of this procedure on each 10-second scan window was visually confirmed alongside the raw pulse oximeter recording to ensure accurate labeling of each heartbeat within that 10-second window.

We obtained the resting heart rate for each subject by applying this procedure to the pulse oximeter recording from each subject's resting scan. Likewise, we applied this procedure to the output from each Focused Awareness task scan and took the average of the three scans to obtain overall heart rate during the task. To calculate average heart rate during heartbeat interoception trials, we ran this procedure only on the 10-second time period corresponding to each heartbeat interoception trial during the Focused Awareness task scans and then calculated the average heart rate during those periods.

Imaging Scan Parameters

We used the following echo-planar imaging (EPI) imaging parameters for the three task scanning runs: field of view (FOV)/slice/gap = 240/2.9/0 mm, axial slices per volume = 46, acquisition matrix = 96 × 96, repetition/echo time TR/TE = 2500/30 ms, SENSE acceleration factor R = 2 in the phase encoding (anterior-posterior) direction, flip angle = 90°, sampling bandwidth = 250 kHz, number of volumes = 220, scan time = 550 sec. We used the same EPI imaging parameters for the resting-state scan, except for: TE = 25 ms, number of volumes = 180, scan time = 450 sec. All EPI images were reconstructed into a 128 × 128 matrix, in which the resulting fMRI voxel volume was 1.875 × 1.875 × 2.9 mm^3. As demonstrated by measurements of temporal signal-to-noise ratio (TSNR), these scan parameters ensured high image quality and reduced

magnetic susceptibility artifacts within limbic regions, including the orbitofrontal cortex (OFC) and subgenual prefrontal cortex (sgPFC) (see Figure S4). We used a T1-weighted magnetization-prepared rapid gradient-echo sequence with SENSE to provide an anatomical reference for the fMRI analysis. The anatomical scan had the following parameters: FOV = 240 mm, axial slices per volume = 176, slice thickness = 0.9 mm, image matrix = 256 x 256, voxel volume 0.938 x 0.938 x 0.9 mm^3, TR/TE = 5/2.02 ms, acceleration factor R = 2, flip angle = 8º, inversion time TI = 725 ms, sampling bandwidth = 31.25 kHz, scan time = 372 sec.

Data Preprocessing

We registered the anatomical scan to the first volume of the resting-state EPI time-course using AFNI's anatomical-to-epi alignment procedure. We then spatially transformed the anatomical scan to the stereotaxic array of Talairach and Tournoux (1) using AFNI's automated algorithm and the transformation parameters were saved for use later in the preprocessing. We excluded the first 4 volumes of each EPI time-course from data analysis to allow the fMRI signal to reach steady state. Subsequently, we applied a slice timing correction to all EPI volumes. We saved estimates of the transformations necessary to register all EPI volumes to the first volume of the first EPI time-course both for the next step in the preprocessing and also for use in the statistical analyses. We implemented motion correction and spatial transformation of the EPI data in a single image transformation, and resampled all images to a 1.75 x 1.75 x 1.75 mm^3 grid. We then smoothed the EPI data with a 6-mm full-width at half-maximum (FWHM) Gaussian kernel, and normalized the signal intensity for each EPI volume to reflect percent signal change from each voxel's mean intensity across the time-course.

Subject-level Statistical Analyses

The regression model included regressors for each interoceptive attention condition and the exteroception condition. To adjust the model for the shape and delay of the blood oxygenation level-dependent (BOLD) function, we constructed the task regressors by convolution of a gamma-variate function and a boxcar function having a 10-second width (or 5-second width for modeling response periods) beginning at the

onset of each occurrence of the condition. Additionally, the regression model included regressors of non-interest to account for each run's signal mean, linear, quadratic, and cubic signal trends, as well as the 6 normalized motion parameters (3 translations, 3 rotations) computed during the image registration preprocessing.

Resting Scan Preprocessing

For preprocessing of the resting-state scans, we employed a modified version of the ANATICOR method (2), implemented through the AFNI program afni_restproc.py (available in the AFNI binaries distributed through the AFNI website). We excluded the first 4 volumes of the resting state-scan in order to remove T1 effects in the data. We then used a de-spiking interpolation algorithm (AFNI's 3dDespike) to remove any transient signal spikes from the data that might artificially inflate estimates of the correlation among voxels' time-series, followed by slice time correction. We then registered each volume in the resting state EPI time-course to the first volume (which was registered to the anatomical scan). We constructed masks of the subject's ventricles and white matter from the subject's anatomical scan using FreeSurfer (http://surfer.nmr.mgh.harvard.edu/), and eroded each mask slightly to prevent partial volume effects that might include signal from gray matter voxels in the mask. First we calculated the average time course during the resting-state run within the ventricle mask. Next, to produce estimates of the local physiological noise, we calculated for each gray matter voxel the average signal time-course for all white matter voxels within a 1.5 cm radius. We also used the respiration and cardiac traces collected during the resting-state scan to calculate RETROICOR (3) and respiration volume per time (RVT) (4) parameters using the RetroTS.m plugin for MATLAB. We then removed the mean, linear, quadratic, and cubic trends from all the regressors of non-interest described above. In total, the estimates of physiological and non-physiological noise included the 6 motion parameters (3 translations, 3 rotations), the average ventricle signal, the average local white matter signal, and 13 respiration regressors from RETROICOR and RVT. We constructed the predicted time-course for these nuisance variables using AFNI's 3dTfitter program, and then subtracted this predicted time-course from each resting-state voxel time-course, yielding a residual time-course for each voxel. We then

smoothed this residual resting-state time-course with a 6 mm FWHM Gaussian kernel, resampled it to a 1.75 mm x 1.75 mm x 1.75 mm grid, and spatially transformed it to stereotaxic space for all subsequent analyses.

Motion Censoring/Additional Motion Correction

Recently, much attention has been paid to the possibility that uncontrolled subject motion can induce artifactual group differences in resting-state functional connectivity analyses (5; 6). We thus implemented motion-censoring algorithms (a.k.a. “scrubbing”) to guard against this possibility in the present study. In order to remove any additional motion related signal artifacts that were still present after regression of motion parameters, we implemented a censoring technique to identify and remove any time point with motion above a certain predefined threshold. We used the AFNI program 1d_tool.py on the 6 motion parameters created during the volume registration step. The output was a single time series reflecting the Euclidean normalized derivative of the motion parameters. We then thresholded this time series, so that any time point where the derivative was greater than 0.3 (roughly 0.3 mm motion) was censored. We also used the AFNI program 3dToutcount to plot the fraction of voxels within a brain mask per time point that were considered outliers. The source of these outliers could include head motion or miscellaneous signal artifacts. We then censored any time point where greater than 5% of brain voxels were considered outliers. We then combined these lists of censored time points created by both methods to create a list of time points censored by both methods. We provided this combined list to the AFNI program 3dDeconvolve, which removed those time points from consideration during the subsequent regression analysis.

Resting-State Functional Connectivity Analyses

At the subject-level, we constructed the seed time-series for both of the dorsal mid-insula regions of interest (ROIs) identified in the heartbeat interoception contrast (Figure 1) by calculating the average time series during the resting-state scan within the ROIs. Using multiple regression analysis, we produced maps of the time-course correlations (r-values) between both of the seed regions and all other voxels in the

brain. We then transformed these r-values to Z-scores. To identify voxels exhibiting group differences in spontaneous BOLD fluctuations correlated with the insular seed regions, we implemented group-level random effects *t*-tests comparing the Z-scores generated for the healthy subjects against the Z-scores generated for the depressed subjects. We corrected all resulting statistical maps for multiple comparisons at $p < .05$ (using the method described below).

To identify regions where resting-state functional connectivity to the insula was associated with depression severity, we examined the correlation between functional connectivity Z-scores for both insula seed regions and the total Hamilton Depression Rating Scale (HDRS) scores of the depressed subjects. We performed a one-sample *t*-test, using the depressed subjects' HDRS scores entered as a covariate, in order to determine if the correlation coefficient for the relationship between Z-scores and HDRS scores within each voxel was significantly different from 0. Resultant maps were cluster-size corrected for multiple comparisons at $p < .05$ as mentioned below.

Correction for Multiple Comparisons and Anatomical ROI Definitions

All voxel-wise statistical maps created for analysis of task data and resting-state data were corrected for multiple comparisons at $p < .05$ as follows. Within *a priori*-defined regions of interest, we used a voxel-wise *p*-value of .01 and a small-volume correction for multiple comparisons using Monte Carlo simulations of cluster size. Those regions included the insular cortex, the amygdala, the orbitofrontal cortex, the caudate, and the ventromedial prefrontal cortex. Outside of these regions of interest we used a voxel-wise threshold of $p < .001$, combined with Monte Carlo simulations of cluster size. We subsequently applied a mask to all contrast maps (see Figure S4) to ensure that in all brain regions exhibiting group differences in interoception or functional connectivity, the TSNR was greater than 40 (Figure S4), allowing for reliable detection of effects between conditions (7).

The regions-of-interest defined *a priori* in the amygdala and caudate were defined using pre-rendered stereotaxic ROI masks available in AFNI. These ROI masks are part of an anatomical atlas based on probability maps generated for 35 cortical areas (8) and the parcellation of cortical and subcortical structures (of the AFNI

Talairach N27 atlas brain) generated by the FreeSurfer program. The left and right insula region-of-interest masks were also generated by the FreeSurfer program, which we applied to the AFNI Talairach N27 atlas brain.

The anterior OFC ROI was bounded posteriorly by a line drawn at the anterior edge of the genu of the corpus callosum (Y = 32 on the AFNI Talairach N27 atlas brain). The ROI was bounded anteriorly by the frontal pole (Y = 61), and ventrally by the ventral edge of the cortex (at approximately Z = -19). Dorsally, the OFC ROI extended up to the fundus of the transverse orbital sulcus, and medially to the medial edge of the medial orbital gyrus (according to the methods defined by Chiavaras *et al*., 2001 (9)). Laterally, the ROI extended to the edge of the lateral intermediate orbital sulcus or the lateral orbital sulcus, whichever of the two was located more medially.

The ventromedial prefrontal cortex (vmPFC) ROI was bounded anteriorly by a line drawn at the anterior edge of the genu of the corpus callosum (Y = 31 on the AFNI Talairach N27 atlas brain; which ensured that the OFC and vmPFC ROIs did not overlap) and posteriorly by a line drawn at the posterior edge of the genu (Y = 9). The ROI was bounded medially and ventrally by the medial and ventral surfaces of the cortex, respectively. Dorsally, the ROI extended to the fundus of the olfactory sulcus and the corpus callosum. Laterally, the vmPFC ROI extended to the lateral edge of the olfactory sulcus.

Supplemental Results

Demographic and Clinical Characteristics

The demographic and clinical characteristics of the study samples are listed in Table 1. As expected, the healthy and depressed groups differed significantly on measures of depression (HDRS: t_{38} = -12.0, p < .001) and anxiety (Hamilton Anxiety Rating Scale (HARS): t_{38} = -13.6, p < .001). The mean age did not differ significantly between groups (t_{38} = -1.3, p = .20), nor did body mass index (t_{38} = -.3, p = .79).

Resting heart rate, obtained during the resting scan, did not differ between depressed and healthy subjects (t_{38} = .5, p = .63; Table 1). Average heart rate during

the Focused Awareness task also did not differ between subjects (t_{38} = .8, p = .43). Additionally, for both healthy and depressed subjects, heart rate during interoception did not differ from the average heart rate during the task itself (p > .3), nor did heart rate during heartbeat interoception differ between subjects (t_{38} = .9, p = .36).

Focused Awareness Task Ratings

As previously described in the Methods section, subject responses were collected after half of the trials to help ensure subjects remained attentive to the task. Depressed and healthy subjects did not differ significantly in the reported subjective intensity of interoceptive sensations (see Table S1). The groups also did not differ in their accuracy in detecting exteroceptive targets (see Table S1), indicating that any observed group difference during the interoceptive attention condition is unlikely to be attributable to a global deficit in attention in the major depressive disorder (MDD) group.

Comorbidity within MDD Subjects

Nine of the MDD subjects had secondary comorbid anxiety disorders (social phobia n = 4, posttraumatic stress disorder n = 3, simple phobia n = 1, panic disorder n = 1). Depressed subjects with and without secondary comorbid anxiety diagnoses did not differ significantly in mean behavioral measures of anxiety or depression (HDRS: t_{18} = .17, p = .87; HARS: t_{18} = .45, p = .66; Table S7). Nor did the depressed subjects with or without comorbid anxiety disorders differ in activity of the dorsal mid-insula during heart interoception (left dorsal mid-insula: t_{18} = -.18, p = .86; right dorsal mid-insula: t_{18} = -.32, p = .75; Table S8).

We supplemented the ROI analyses mentioned above with whole-brain voxel-wise analyses of the BOLD response during heart, stomach, and bladder interoception. After correction for multiple comparisons, we did not identify any regions of the brain exhibiting significant differences in response between depressed subjects with and without secondary comorbid anxiety diagnoses.

The Hemodynamic Response to Interoception and Other Behavioral Measures

We conducted further analyses of the relationship between the hemodynamic response during interoceptive attention and behavioral measures collected from healthy and depressed subjects.

Focused Awareness task ratings

The hemodynamic response within the dorsal mid-insula cortex (dmIC) during heartbeat interoception was significantly related to healthy subject's ratings of the intensity of heartbeat sensations (Right: $r = -.73$, $p < .001$; Left: $r = -.47$, $p < .04$), but not the ratings made by depressed subjects (Right: $r = .24$, $p = .31$; Left: $r = .07$, $p = .78$). A test of the difference in slopes of these relationships revealed that depressed and healthy subjects differed significantly in the relationship between right dmIC activity and heartbeat intensity ratings ($t = -2.51$, $p < .02$).

Subsequently, we conducted a whole-brain voxel-wise analysis to locate other brain regions exhibiting similar group differences in the relationship between heartbeat intensity ratings and BOLD response during heartbeat interoception. After correction for multiple comparisons, the right dmIC (Talairach coordinate: 38, -4, 11) was the only region of the brain that exhibited significant group differences in this relationship. The activation cluster within this group analysis was spatially contiguous with the right dmIC cluster where group differences in the magnitude of the hemodynamic response to heartbeat interoception were first observed (Figure 1).

Major depressive episode duration

ROI analysis results: We did not observe any significant correlations between dmIC task activation and major depressive episode duration in the depressed subjects (Table S9).

Somatic symptom severity

Voxel-wise analysis results: Depressed subjects exhibited a significant negative correlation between BOLD activity during heartbeat interoception and somatic symptom severity, as measured by the HDRS somatic symptom sub-scale (10), within bilateral amygdala and medial OFC (Table S10).

Anxiety severity

ROI analysis results: Within the depressed subjects, we observed no significant correlation between HARS scores and task activation within either dmIC cluster (Table S3).

Voxel-wise analysis results: After applying corrections for multiple comparisons, we did not observe any region of the brain that showed a significant relationship between activation during heartbeat interoception and anxiety, as measured by the HARS.

Additionally, using the AFNI program 3dttest++, we re-ran the whole-brain voxel-wise analysis of group differences in heartbeat interoception between depressed and healthy subjects (Figure 1, Table 2), this time including HARS severity scores as a covariate of no interest. The results of this analysis were almost identical to the results of the original analysis (e.g., see Figure 1, Table 2). All of the brain regions previously identified within this contrast were present after including the HARS covariate, though in some cases those regions were larger or smaller by a small number of voxels.

Functional Connectivity of the dmIC and Other Behavioral Measures

Somatic symptom severity

Depressed subjects exhibited a significant positive correlation between left dmIC functional connectivity and somatic symptom severity, as measured by the HDRS somatic symptom sub-scale (10), within right amygdala and right sgPFC (Table S11). After correction for multiple comparisons, no brain regions exhibited a significant correlation between right dmIC functional connectivity and somatic symptom severity.

Anxiety severity

After applying corrections for multiple comparisons, we did not observe any region of the brain that showed a significant relationship between dmIC functional connectivity and anxiety, as measured by the HARS.

Additional Group Differences in Stomach and Bladder Interoception

Having identified that depressed subjects also exhibit decreased dmIC response to stomach and bladder interoception within the dmIC, we subsequently conducted

whole-brain group analyses comparing the hemodynamic response to stomach and bladder interoception between groups. The analyses were conducted as described in the methods section of the main paper, and both contrast maps were corrected for multiple comparisons as described above in the Supplemental Methods.

As expected, depressed subjects exhibited significantly decreased hemodynamic activity compared to healthy subjects within multiple other brain regions during attention to stomach and bladder sensations (Figure S5, Table S12), including many regions also observed within the heartbeat interoception contrast (Figure 1). Group differences in stomach and bladder interoception were observed in ventral mid-insula, a region previously identified along with dmIC as functionally selective for interoceptive attention, as well as the amygdala and OFC. Depressed subjects also exhibited decreased hemodynamic response within right dorsal anterior insula, involved in salience processing and focal attention (11; 12), as well as the right precuneus, a component of the default mode network (13), during stomach interoception.

Supplemental Discussion

Depression, Anxiety, and Interoceptive Awareness

Previous research suggests that both anxiety and depression play a part in modulating interoceptive awareness (14; 15). Some evidence suggests that anxiety and depression lie at opposite ends along a continuum of interoceptive awareness, with anxiety as a positive modulator and depression as a negative modulator (14). For example, trait anxiety has been associated with increased heartbeat perception accuracy (16) and panic disorder with increased sensitivity to anxiogenic challenge by sodium lactate infusion and 35% CO2 inhalation (17; 18). Depression, on the other hand, has been associated with decreased interoceptive accuracy and decreased heartbeat-evoked potential (14; 19).

However, due to the frequent comorbidity of mood and anxiety disorders (20), this relationship becomes much more complicated. The negative relationship between heartbeat perception accuracy and depression held only at high anxiety levels (14), and

depression-specific symptoms seem to modulate the relationship between anxiety and interoception (21). Additionally, though recent studies have attempted to account for this factor by recruiting depressed subjects with no comorbid anxiety disorders, those subjects still report significantly higher levels of anxiety than controls (22). One possible explanation for these discrepant findings comes from the hypothesis that, rather than considering anxiety and depression to be two distinct conditions, major depressive episodes occur as an adaptive, homeostatic response, possibly to chronically high levels of anxiety (23). In this scenario, the acute state of depression, with its accompanying physiological changes, such as decreased parasympathetic regulation of cardiac tone (24) and decreased baroreceptor sensitivity (25), conceivably may result in decreased interoceptive awareness, regardless of the presence of anxiety. However, this does not entirely preclude the effect of anxiety, as higher levels of chronic anxiety conceivably may lead to more severe depression and thus result in a greater decrease in interoceptive awareness.

In this study, depressed subjects both with and without comorbid anxiety disorders had significantly higher levels of both anxiety and depressive symptoms than controls, accompanied by significantly decreased dmIC activation during interoceptive attention. Within MDD subjects, severity of depression (as rated by the HDRS scores) negatively correlated with activation during heartbeat interoception within the insula, as well as with resting state functional connectivity between the insula and depression-associated brain regions. A subsequent analysis using sub-scales of the HDRS (10) revealed that the relationship between heartbeat interoception and depression severity was strongly driven by the severity of somatic symptoms in depressed subjects. Importantly, behavioral measures of anxiety alone did not significantly modulate heartbeat interoception; neither did the presence of comorbid anxiety disorders among the MDD subjects. This suggests that, within these subjects, the hemodynamic activity within the insula during visceral interoception is most strongly associated with the somatic symptoms that accompany major depression.

The Focused Awareness Task

The Focused Awareness task originally was designed to identify areas of the insula selectively responsive for cognitive, sensory, and emotional processes, in an attempt to reconcile patterns of activation reported across various studies that overlap within the same regions of the insula. Neuroimaging studies of gustation (a sensory modality that shares a common neural pathway with vagal afferents from the heart and viscera (26)) also frequently report a variability in the location of gustatory activation within the insula, dependent on the specific cognitive requirements of the task (27; 28). The Focused Awareness task thus was designed so that participants would passively attend to the sensations from their heart and viscera, in order to directly isolate primary viscerosensory regions of the insula, without the confounding demands of other cognitive tasks, such as exteroceptive attention to compare heartbeats against external auditory tones. The results of the Focused Awareness task bear this out, as attention to heart and stomach sensations selectively activated regions of the mid-insula identified through cytoarchitecture, anatomical studies, and neuroimaging meta-analyses as primary viscerosensory areas of the insula (26; 29-32).

Through this method, we are able to identify group differences in activation during interoceptive *attention* within these primary sensory regions of the insula, though the very nature of the task precludes the ability to identify group differences in interoceptive *accuracy*. Within the current study, the self-report ratings made by subjects after interoceptive attention trials relate specifically to the subjective intensity of their experience during the preceding trial, and were primarily included to ensure that subjects remained attentive to the task. Our comparisons of intensity ratings between groups were done in order to confirm that both depressed and healthy subjects performed the task equivalently. Given that these ratings were not measures of objective interoceptive accuracy, the lack of group differences in the magnitude of these ratings does not noticeably contradict findings from previous studies measuring heartbeat perception accuracy in depression (19; 22; 33; 34).

The lack of an external accuracy measure for interoceptive trials makes it difficult to verify objectively that all subjects performed the task equivalently. However, analysis of post-trial rating periods, during which subjects reported the subjective intensity of

interoceptive sensations or the number of targets presented, allows us to demonstrate that the two groups performed the exteroception tasks equally well and rated the interoceptive sensations as having equal intensity (see Supplemental Results section). In post-scan interviews, all MDD and healthy control subjects reported both understanding and performing the interoception task.

Additionally, we have demonstrated in a separate study that the accuracy of subjects' interoceptive perceptions is correlated with the activity of the mid-insula during this same interoception task used in the present study (35). This gives us even more confidence that MDD participants are performing the interoception task as instructed, and that the activity of this region is related to interoceptive awareness.

Analysis of the Focused Awareness task data within this study revealed group differences within a specific region of the insula, previously identified as selective for visceral interoception. In depressed subjects, activity within this region during heartbeat interoception was correlated with the severity of their depression (r = -.44; p = .05) as well as the severity of their somatic symptoms (r = -.53; p = .02). Likewise, in depressed subjects, the functional connectivity between this region and limbic brain regions such as the amygdala also correlated with depression severity (Figure S3). These findings all indicate that the results of this study accurately reflect depression-related effects on the cortical representation of visceral interoception.

Table S1. Focused Awareness task ratings

	HC Mean (SD)	MDD Mean (SD)	t_{38}	*p*
Intensity Ratings				
Heart	4.08 (1.75)	4.31 (1.50)	-.45	.66
Stomach	4.6 (1.57)	4.88 (1.50)	-.58	.56
Bladder	5.06 (1.66)	4.29 (1.81)	1.40	.17
Target Detection Accuracy				
% Accuracy	90.0 (15.7)	85.5 (13.5)	.96	.34

HC, healthy controls; MDD, major depressive disorder subjects.

Table S2. Group differences in dmIC activity during stomach and bladder interoception

	Healthy Subjects % signal change			MDD Subjects % signal change			HC-MDD	
	Mean (SD)	t_{19}	*p*	Mean (SD)	t_{19}	*p*	t_{38}	*p*
L dmIC								
Stomach	.028 (.02)	7.26	<.001	.010 (.02)	2.17	.04	2.99	.005
Bladder	.023 (.02)	4.59	<.001	.005 (.02)	.84	.41	2.52	.02
R dmIC								
Stomach	.031 (.02)	6.99	<.001	.014 (.03)	2.00	.06	1.99	.05
Bladder	.029 (.03)	3.87	.001	.008 (.03)	1.06	.30	1.97	.06

dmIC, dorsal mid-insula cortex; HC, healthy controls; L, left; MDD, major depressive disorder subjects; R, right.

Table S3. Correlation of dmIC activity during interoception with total HDRS and HARS rating scale scores in the depressed subjects

	HDRS		HARS	
	r_{18}	*p*	r_{18}	*p*
L dmIC				
Heart	-.44	.05	-.23	.33
Stomach	-.18	.45	-.13	.58
Bladder	-.31	.18	-.27	.26
R dmIC				
Heart	-.31	.18	-.10	.68
Stomach	.14	.56	-.02	.94
Bladder	-.03	.92	-.12	.62

dmIC, dorsal mid-insula cortex; HARS, Hamilton Anxiety Rating Scale; HDRS, Hamilton Depression Rating Scale; L, left; MDD, major depressive disorder subjects; R, right.

Table S4. Correlation of dmIC activity during heartbeat interoception with HDRS sub-scales in depressed subjects from (Cleary and Guy, (10))

	L dmIC		R dmIC	
HDRS Factor	r_{18}	*p*	r_{18}	*p*
Anxiety/Somatization	**-.53**	**.02**	-.41	.07
Weight Loss[a]	--	--	--	--
Cognitive Disturbance	.03	.90	<.01	>.99
Diurnal Variation	.03	.90	-.12	.61
Retardation	-.13	.59	-.03	.89
Sleep Disturbance	-.06	.81	-.01	.95

[a] The Weight Loss factor from Cleary and Guy (10) was excluded as no subjects reported significant weight changes.

Bolded values indicate significance.

dmIC, dorsal mid-insula cortex; HDRS, Hamilton Depression Rating Scale; L, left; R, right.

Table S5. Brain regions where the hemodynamic response to heartbeat interoception was correlated with depression severity[a]

Side / Location	Peak Coordinates[b]			t_{38}	Volume
	X	Y	Z		(mm^3)
L Amygdala	-25	-4	-19	-4.54	1549
L Ventral Anterior Insula	-36	+10	-7	-5.58	1184
L Posterior OFC (BA13a)	-10	+13	-10	-4.69	997
L Superior Parietal Lobule	-24	-55	+39	-6.90	590
L Middle Occipital Gyrus[c]	-29	-69	+21	-5.45	557
L Ventral and Dorsal Mid-Insula	-36	-4	2	-3.60	214
R Amygdala	+18	+1	-17	-3.44	107

[a] Within the depressed subjects.

[b] All coordinates reported according to Talairach stereotaxic atlas (1). This format uses three numbers (X,Y,Z) to describe the distance from the anterior commissure. The X,Y,Z dimensions refer to right(+)-to-left(-), anterior(+)-to-posterior(-), and dorsal(+)-to-ventral(-) respectively.

BA, Brodmann area; L, left; OFC, orbitofrontal cortex; R, right.

Table S6. Brain regions where functional connectivity with the dmIC was correlated with depression severity

Side / Location	Peak Coordinates[a]			t_{18}	Volume
	X	Y	Z		(mm^3)
Left dmIC Seed					
R Posterior OFC (BA13a)	+10	+22	-8	4.94	879
R Subgenual PFC (BA32pl)					
R Medial OFC (BA11l/m)	+22	+55	-8	4.60	573
L Ventral Mid-Insula	-39	-3	-14	4.79	498
L Posterior OFC (BA13a)	-8	+17	-12	4.69	466
L Subgenual PFC (BA32pl)					
R Supramarginal Gyrus	+34	-52	+27	5.99	391
R Ventral Posterior Insula	-38	-19	+2	3.86	381
L Middle Temporal Gyrus	-52	-40	-3	5.13	279
L Amygdala	-18	+4	-14	3.63	166
L Medial OFC (BA11l/m)	-15	+52	-10	4.26	150
Right dmIC Seed					
R Ventral Anterior Insula	+36	+11	-5	5.04	1201
R Medial OFC (BA11l/m)	+22	+48	-7	5.34	1120
L Posterior OFC (BA13a)	-18	+8	-12	4.71	900
R Inferior Frontal Gyrus	+46	+22	+13	6.13	718
L Ventral Mid-Insula	-36	-1	-12	4.30	488
R Ventral Posterior Insula	-38	-15	-1	4.14	343
R Superior Frontal Gyrus	+20	+52	+25	4.96	241
L Ventral Anterior Insula	-34	+15	-1	4.03	230
L Subgenual PFC (BA32pl)	-4	+20	-12	4.00	204
L Medial OFC (BA11l/m)	-20	+39	-12	3.87	123
R Posterior OFC (BA13a)	+13	+18	-17	3.26	113
L Medial OFC (BA11l/m)	-13	+52	-8	3.76	86

[a] All coordinates reported according to Talairach stereotaxic atlas (1). This format uses three numbers (X,Y,Z) to describe the distance from the anterior commissure. The X,Y,Z dimensions refer to right(+)-to-left(-), anterior(+)-to-posterior(-), and dorsal(+)-to-ventral(-) respectively.

BA, Brodmann area; dmIC, dorsal mid-insula cortex; L, left; OFC, orbitofrontal cortex; PFC, prefrontal cortex; R, right.

Table S7. Comparison of MDD subjects with and without secondary comorbid anxiety diagnoses

	Demographics			
	MDD w/o comorbid	**MDD w/ comorbid**	t_{18}	***p*-value**
HDRS	23.6 (7.9)	23.0 (8.8)	.17	.87
HARS	17.5 (5.3)	16.4 (4.4)	.45	.66

HARS, Hamilton Anxiety Rating Scale; HDRS, Hamilton Depression Rating Scale; MDD, major depressive disorder subjects; w/, with; w/o, without.

Table S8. Comparison of dmIC activity during heartbeat interoception between MDD subjects with and without comorbid anxiety disorders

	MDD w/o comorbid			**MDD w/ comorbid**			**$MDD_{w/o}$-$MDD_{w/}$**	
	% signal change			**% signal change**				
	Mean (SD)	t_{10}	***p***	**Mean (SD)**	t_8	***p***	t_{18}	***p***
L dmIC	-.0004 (.03)	-.04	.97	-.003 (.03)	-.27	.79	.18	.86
R dmIC	-.002 (.04)	-.15	.88	.003 (.03)	.31	.76	-.32	.75

dmIC, dorsal mid-insula cortex; L, left; MDD, major depressive disorder subjects; R, right; w/, with; w/o, without.

Table S9. Correlation of dmIC activity during interoception with MDE duration in the depressed subjects

	L dmIC		**R dmIC**	
	r_{18}	***p***	r_{18}	***p***
Heart	-0.13	.60	-0.12	.60
Stomach	0.21	.38	0.12	.60
Bladder	0.22	.36	0.15	.51

dmIC, dorsal mid-insula cortex; L, left; MDE, major depressive episode; R, right.

Table S10. Brain regions where the hemodynamic response to heartbeat interoception was correlated with somatic symptom severity[a]

Side / Location	Peak Coordinates[b]			t_{18}	Volume
	X	Y	Z		(mm^3)
R Amygdala	+18	-1	-17	-3.60	140
R Medial OFC (BA11m)	+11	+25	-12	-3.87	140
L Amygdala	+18	+1	-17	-3.44	118

[a] Within the depressed subjects, assessed by the somatic subscale of the HDRS, developed by Cleary and Guy (10).

[b] All coordinates reported according to Talairach stereotaxic atlas (1). This format uses three numbers (X,Y,Z) to describe the distance from the anterior commissure. The X,Y,Z dimensions refer to right(+)-to-left(-), anterior(+)-to-posterior(-), and dorsal(+)-to-ventral(-) respectively.

BA, Brodmann area; HDRS, Hamilton Depression Rating Scale; L, left; OFC, orbitofrontal cortex; R, right.

Table S11. Brain regions where functional connectivity with the dmIC was correlated with somatic symptom severity[a]

Side / Location	Peak Coordinates[b]			t_{18}	Volume
	X	Y	Z		(mm^3)
Left dmIC Seed					
R Amygdala	+22	-1	-24	4.68	118
R Subgenual PFC (BA32pl)	+4	+15	-14	4.26	102

[a] Within the depressed subjects, assessed by the somatic subscale of the HDRS, developed by Cleary and Guy (10).

[b] All coordinates reported according to Talairach stereotaxic atlas (1). This format uses three numbers (X,Y,Z) to describe the distance from the anterior commissure. The X,Y,Z dimensions refer to right(+)-to-left(-), anterior(+)-to-posterior(-), and dorsal(+)-to-ventral(-) respectively.

BA, Brodmann area; dmIC, dorsal mid-insula cortex; HDRS, Hamilton Depression Rating Scale; PFC, prefrontal cortex; R, right.

Table S12. Brain regions exhibiting differences in the hemodynamic response to stomach and bladder interoception between healthy and depressed subjects[a]

Side / Location	Peak Coordinates[b]			t_{18}	Volume
	X	Y	Z		(mm^3)
Bladder Interoception					
R Claustrum	+36	-10	-1	3.70	162
R Putamen					
R Lateral OFC (BA11l)	+22	+32	-10	3.70	123
R Ventral Mid-Insula	+48	+2	-3	3.46	86
R Posterior OFC (BA13a)	+20	+13	-15	4.59	45
R Amygdala	+20	-1	-10	3.52	42
Stomach Interoception					
Right OFC (BA11/13)	+16	+32	-10	5.17	6287
Left Superior Parietal Lobule	-29	-50	+42	5.09	1410
Left Middle Occipital Gyrus	-48	-66	-3	4.53	1088
Right Precuneus	+6	-64	+46	4.64	874
Right Cerebellum	-6	-76	-17	4.67	858
Left Precentral Gyrus	-17	-8	+44	4.83	831
Left Ventral Anterior and Mid Insula	-38	+6	-3	4.81	670
Right Ventral Mid Insula	+36	+4	-7	4.22	665
Left Inferior Parietal Lobule	-50	-29	+37	4.56	638
Right Mid Cingulate Gyrus	+11	-15	+30	5.20	616
Right Claustrum	+34	-17	+0	4.33	391
Right Dorsal Anterior Insula	+36	+22	+6	3.68	370
Left Amygdala					

[a] In all cases, activity was greater in healthy subjects compared to the MDD group.

[b] All coordinates reported according to Talairach stereotaxic atlas (1). This format uses three numbers (X,Y,Z) to describe the distance from the anterior commissure. The X,Y,Z dimensions refer to right(+)-to-left(-), anterior(+)-to-posterior(-), and dorsal(+)-to-ventral(-) respectively.

BA, Brodmann area; MDD, major depressive disorder; OFC, orbitofrontal cortex; R, right.

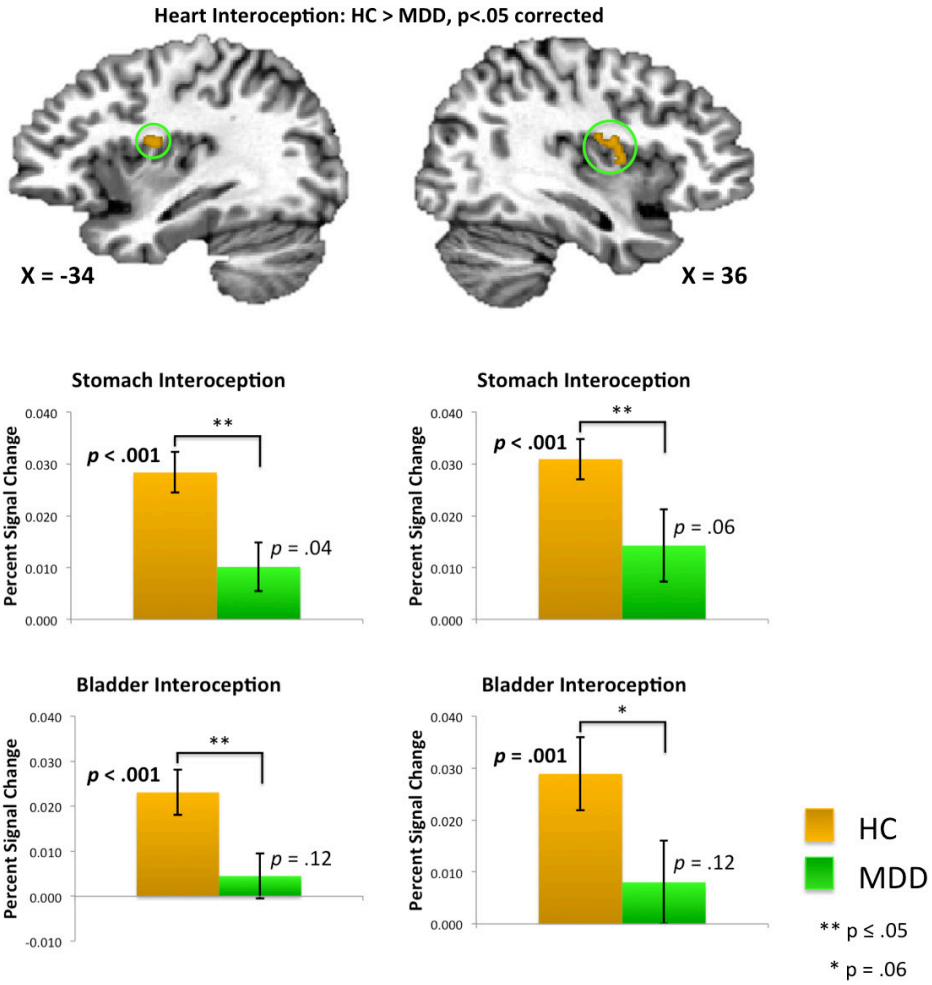

Figure S1. Group differences in stomach and bladder Interoception. Healthy participants (yellow bar) exhibited significantly greater activation within the dmIC ROIs – which were identified in the heartbeat interoception contrast (Figure 1) - during stomach and bladder interoception than during the exteroceptive control condition. In most cases, the depressed participants (green bar) exhibited reliably less activation during stomach and bladder interoception than the healthy subjects. Importantly, within this region of the insula, healthy and depressed subjects did not differ in activation during the exteroceptive control condition (Left ROI: p = 0.18, Right ROI: p = 0.23). HC, healthy controls; MDD, major depressive disorder subjects.

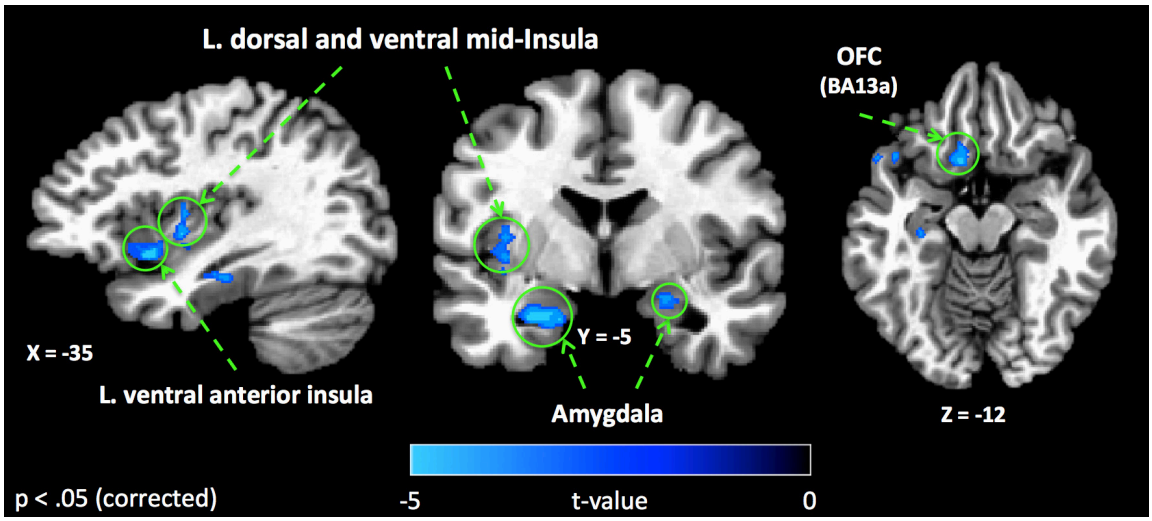

Figure S2. Brain regions where activation during heartbeat interoception is correlated with depression severity. Depressed subjects exhibited a significant negative correlation between hemodynamic activity during heartbeat interoception and scores on the Hamilton Depression Rating Scale within left ventral anterior and ventral and dorsal mid-insula, as well as right posterior OFC and bilateral amygdala. All results shown were corrected for multiple comparisons at $p_{corrected} < .05$. BA, Brodmann area; L., left; OFC, orbitofrontal cortex.

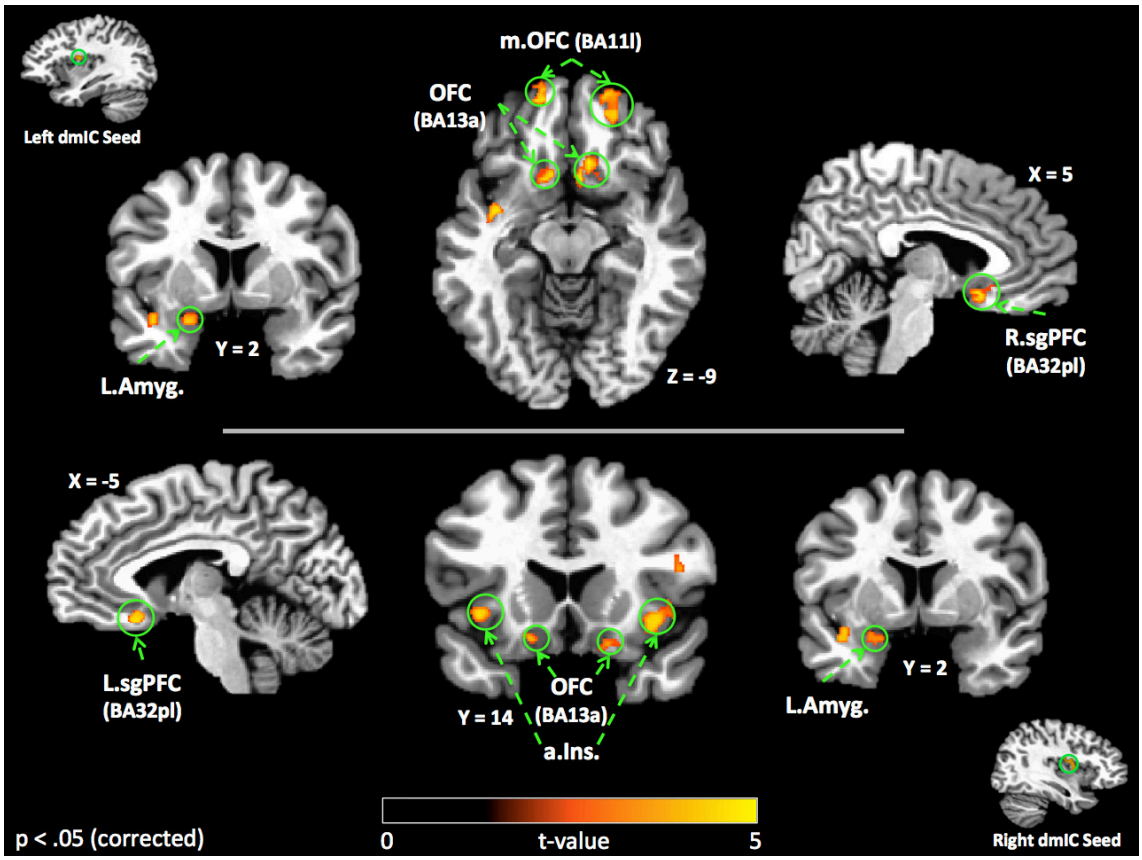

Figure S3. Dorsal mid-insula resting-state functional connectivity is correlated with depression severity. This figure shows the brain regions where resting-state functional connectivity to the dmIC was significantly correlated with depression severity. Many of these regions, notably the left amygdala and regions of the orbitofrontal cortex, also exhibited significant group differences in functional connectivity to the dmIC (see Figure 3). All results corrected for multiple comparisons at $p_{corrected} < .05$. a.Ins., anterior insula; Amyg., amygdala; BA, Brodmann area; dmIC, dorsal mid-insula cortex; L., left; m., medial; OFC, orbitofrontal cortex; R., right; sgPFC, subgenual prefrontal cortex.

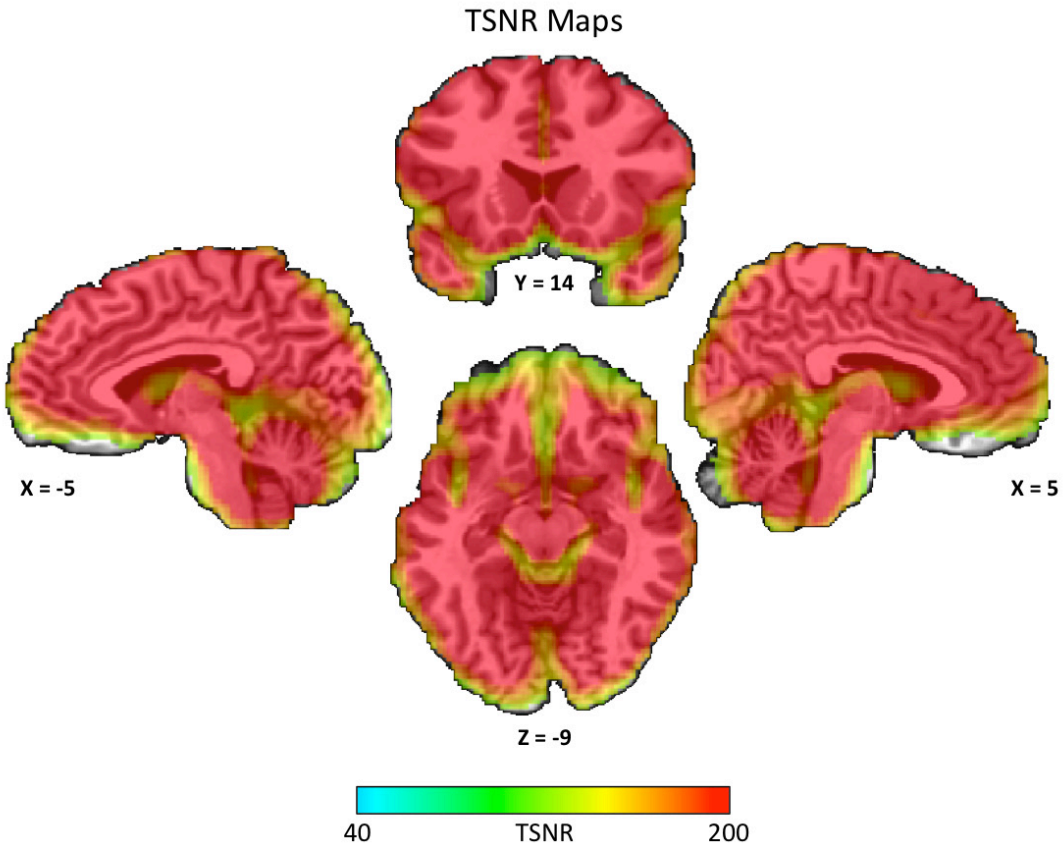

Figure S4. Temporal signal-to-noise ratio (TSNR) maps. These maps depict the TSNR of the smoothed echo-planar imaging time course data acquired in this study. TSNR was calculated by dividing each voxel's mean signal intensity by the standard deviation of the residual time-course, obtained by subtracting the regression model from the signal time-course. All colored areas shown have TSNR of at least 40, the minimum to reliably detect effects between conditions in fMRI data (7). All the figures in this text are displayed strictly within a mask where TSNR > 40.

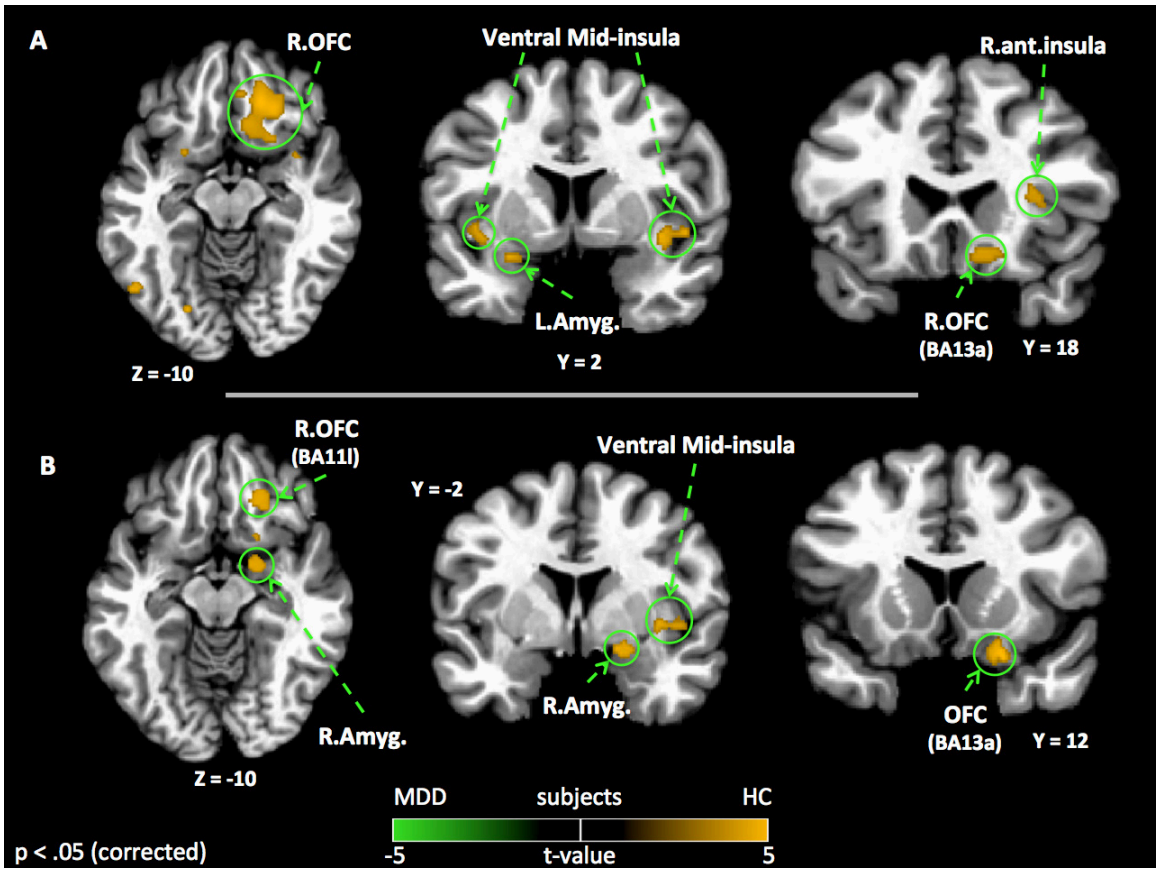

Figure S5. Group differences in stomach and bladder interoception. Outside of the dmIC, depressed subjects exhibited decreased hemodynamic activity compared to healthy subjects within multiple other brain regions during attention to stomach and bladder sensations (**A**: Stomach Interoception, **B**: Bladder Interoception). Group differences in stomach and bladder interoception were observed in ventral mid-insula and right OFC, as well as right and left amygdala. Depressed subjects also exhibited decreased hemodynamic response within right dorsal anterior insula during stomach interoception. All results shown were corrected for multiple comparisons at $p_{corrected} < .05$. Amyg., amygdala; ant., anterior; BA, Brodmann area; dmIC, dorsal mid-insula cortex; HC, healthy controls; L, left; MDD, major depressive disorder subjects; OFC, orbitofrontal cortex; R., right.

Supplemental References

1. Talairach J, Tournoux JTP (1988): *Co-planar Stereotaxic Atlas of the Human Brain*. New York: Thieme Medical Publishers.

2. Jo HJ, Saad ZS, Simmons WK, Milbury LA, Cox RW (2010): Mapping sources of correlation in resting state FMRI, with artifact detection and removal. *Neuroimage* 52: 571–582.

3. Glover GH, Li T-Q, Ress D (2000): Image-based method for retrospective correction of physiological motion effects in fMRI: RETROICOR. *Magn Reson Med* 44: 162–167.

4. Birn RM, Murphy K, Bandettini PA (2008): The effect of respiration variations on independent component analysis results of resting state functional connectivity. *Hum Brain Mapp* 29: 740–750.

5. Power JD, Barnes KA, Snyder AZ, Schlaggar BL, Petersen SE (2012): Spurious but systematic correlations in functional connectivity MRI networks arise from subject motion. *Neuroimage* 59: 2142–2154.

6. Saad ZS, Gotts SJ, Murphy K, Chen G, Jo HJ, Martin A, Cox RW (2012): Trouble at rest: how correlation patterns and group differences become distorted after global signal regression. *Brain Connect* 2: 25–32.

7. Murphy K, Bodurka J, Bandettini PA (2007): How long to scan? The relationship between fMRI temporal signal to noise ratio and necessary scan duration. *Neuroimage* 34: 565–574.

8. Desikan RS, Ségonne F, Fischl B, Quinn BT, Dickerson BC, Blacker D, *et al.* (2006): An automated labeling system for subdividing the human cerebral cortex on MRI scans into gyral based regions of interest. *Neuroimage* 31: 968–980.

9. Chiavaras MM, Legoualher G, Evans A, Petrides M (2001): Three-dimensional probabilistic atlas of the human orbitofrontal sulci in standardized stereotaxic space. *Neuroimage* 13: 479–496.

10. Cleary P, Guy W (1977): Factor analysis of the Hamilton depression scale. *Drugs Exp Clin Res* 1: 115–120.

11. Bud Craig AD (2009): How do you feel — now? The anterior insula and human awareness. *Nat Rev Neurosci* 10: 59–70.

12. Nelson SM, Dosenbach NUF, Cohen AL, Wheeler ME, Schlaggar BL, Petersen SE (2010): Role of the anterior insula in task-level control and focal attention. *Brain Struct Funct* 214: 669–680.

13. Li B, Liu L, Friston KJ, Shen H, Wang L, Zeng L-L, Hu D (2013): A treatment-resistant default mode subnetwork in major depression. *Biol Psychiatry* 74: 48–54.

14. Pollatos O, Traut-Mattausch E, Schandry R (2009): Differential effects of anxiety and depression on interoceptive accuracy. *Depress Anxiety* 26: 167–173.

15. Paulus MP, Stein MB (2010): Interoception in anxiety and depression. *Brain Struct Funct* 214: 451–463.

16. Domschke K, Stevens S, Pfleiderer B, Gerlach AL (2010): Interoceptive sensitivity in anxiety and anxiety disorders: An overview and integration of neurobiological findings. *Clin Psychology Rev* 30: 1–11.

17. Johnson PL, Truitt W, Fitz SD, Minick PE, Dietrich A, Sanghani S, *et al.* (2010): A key role for orexin in panic anxiety. *Nat Med* 16: 111–115.

18. Perna G, Barbini B, Cocchi S, Bertani A, Gasperini M (1995): 35% CO2 challenge in panic and mood disorders. *J Affect Disord* 33: 189–194.

19. Terhaar J, Viola FC, Bär K-J, Debener S (2012): Heartbeat evoked potentials mirror altered body perception in depressed patients. *Clin Neurophysiol* 123: 1950–1957.

20. Gorman JM (1996): Comorbid depression and anxiety spectrum disorders. *Depress Anxiety* 4: 160–168.

21. Dunn BD, Stefanovitch I, Evans D, Oliver C, Hawkins A, Dalgleish T (2010): Can you feel the beat? Interoceptive awareness is an interactive function of anxiety- and depression-specific symptom dimensions. *Behav Res Ther* 48: 1133–1138.

22. Furman DJ, Waugh CE, Bhattacharjee K, Thompson RJ, Gotlib IH (2013): Interoceptive awareness, positive affect, and decision making in Major Depressive Disorder. *J Affect Disord* 151: 780–785.

23. Andrews PW, Kornstein SG, Halberstadt LJ, Gardner CO, Neale MC (2011): Blue again: perturbational effects of antidepressants suggest monoaminergic homeostasis in major depression. *Front Psychol* 2: 159.

24. Carney RM, Blumenthal JA, Freedland KE, Stein PK, Howells WB, Berkman LF, *et al.* (2005): Low heart rate variability and the effect of depression on post-myocardial infarction mortality. *Arch Intern Med* 165: 1486–1491.

25. Broadley AJM, Frenneaux MP, Moskvina V, Jones CJH, Korszun A (2005): Baroreflex sensitivity is reduced in depression. *Psychosom Med* 67: 648–651.

26. Craig AD (2002): How do you feel? Interoception: the sense of the physiological condition of the body. *Nat Rev Neurosci* 3: 655–666.

27. Small DM (2010): Taste representation in the human insula. *Brain Struct Funct* 214: 551–561.

28. Veldhuizen MG, Albrecht J, Zelano C, Boesveldt S, Breslin P, Lundström JN (2011): Identification of human gustatory cortex by activation likelihood estimation. *Hum Brain Mapp* 32: 2256–2266.

29. Morel A, Gallay MN, Baechler A, Wyss M, Gallay DS (2013): The human insula: Architectonic organization and postmortem MRI registration. *Neuroscience* 236: 117–135.

30. Proserpio P, Cossu M, Francione S, Tassi L, Mai R, Didato G, *et al.* (2011): Insular-opercular seizures manifesting with sleep-related paroxysmal motor behaviors: a stereo-EEG study. *Epilepsia* 52: 1781–1791.

31. Kurth F, Zilles K, Fox PT, Laird AR, Eickhoff SB (2010): A link between the systems: functional differentiation and integration within the human insula revealed by meta-analysis. *Brain Struct Funct* 214: 519–534.

32. Kelly C, Toro R, Di Martino A, Cox CL, Bellec P, Castellanos FX, Milham MP (2012): A convergent functional architecture of the insula emerges across imaging modalities. *Neuroimage* 61: 1129–1142.

33. Dunn BD, Dalgleish T, Ogilvie AD, Lawrence AD (2007): Heartbeat perception in depression. *Behav Res Ther* 45: 1921–1930.

34. Mussgay L, Klinkenberg N, Rüddel H (1999): Heart beat perception in patients with depressive, somatoform, and personality disorders. *J Psychophysiol* 13: 27–36.

35. Kleckner IR, Avery JA, Quigley KS, Simmons WK, Barrett LF (2013, October 28): Neural correlates of interoceptive attention and interoceptive accuracy. *Cognitive Neuroscience Society.* San Francisco, CA.